Geochemical and radiogenic isotopic signatures of granitic rocks in Chanthaburi and Chachoengsao provinces, southeastern Thailand: Implications for origin and evolution

Etsuo Uchida [a,*], Shinya Nagano [a], Sota Niki [b], Kou Yonezu [a], Yu Saitoh [a], Ki-Cheol Shin [c], Takafumi Hirata [b]

[a] *Department of Resources and Environmental Engineering, School of Creative Science and Engineering, Waseda University, Shinjuku-ku, Tokyo 169-8555, Japan*
[b] *Geochemical Research Center, Graduate School of Science, The University of Tokyo, Hongo 7-3-1, Bunkyo-ku, Tokyo 113-0064, Japan*
[c] *Research Institute for Humanity and Nature, Kamigamo 457-4, Kita-ku, Kyoto 603-8047, Japan*

ABSTRACT

The Chanthaburi, Pliew, Klathing, Khao Cha Mao, and Khao Hin Son granitic bodies in Chanthaburi and Chachoengsao provinces in southeastern Thailand, which are located on the southwestern side of the Mae Ping Fault and eastern side of the Klaeng Fault, were investigated. In this study, magnetic susceptibility measurements, whole-rock chemical composition and Nd-Sr isotope analyses, and zircon U-Pb dating were conducted on these granitic bodies. The surveyed granitic rocks are classified as I- to A-type granites, are of the ilmenite series, and show clearly negative Eu anomalies, which suggest they formed under reducing conditions. Nd-Sr isotope ratios indicate continental crust material involvement in the formation of these granite bodies. The magnetic and geochemical signatures are similar to those of granite bodies in southwestern Cambodia. The study area is thus considered an extensional area of southwestern Cambodia, corresponding to the Sukhothai Zone (the Chanthaburi-Kampong Chhnang Zone). Zircon U-Pb dating yields ages of 208–214 Ma (the Late Triassic) for granite bodies except for the Khao Cha Mao granitic body, which dates to 55 Ma. The former age corresponds to the collision time of the Sibumasu and Indochina terranes, and the latter age is likely related to the collision time of the Indian and Eurasian continents.

1. Introduction

The history of tectonic development in mainland Southeast Asia can be roughly explained by the collision between the South China, Indochina, Sibumasu (defined by Metcalfe, 1984), West Myanmar, and Indian Continent terranes which were separated from the margin of Eastern Gondwana (e.g., Sone and Metcalfe, 2008; Ferrari et al., 2008; Sanematsu et al., 2011; Metcalfe, 2011, 2013; Searle et al., 2012; Morley, 2012; Morley et al., 2013; Shellnutt et al., 2013; Burrett et al., 2014; Kamvong et al, 2014; Khin Zaw et al., 2014; Manaka et al., 2014; Gardinier et al., 2015; Wang et al., 2016; Faure et al., 2018; Rossignol et al., 2018; Shi et al., 2021). There were three Tethyan Oceans, the Paleo-Tethys, Meso-Tethys and Ceno-Tethys among the above mentioned terranes. However, the details of tectonic settings of these terranes remain controversial.

Granitic rocks are widely distributed in Thailand and occur in eastern, central, and western granite belts (Cobbing et al., 1986; Charusiri et al., 1993). The eastern granite belt belongs to the Indochina terrane and is characterized by I-type granites, and central and western granite belts belong to the Sibumasu terrane and is characterized by S-type granite (Charusiri et al., 1993). The Indochina terrane is bounded by the Changning-Menglian, Inthanon and Bentong-Raub suture zones in the west (e.g., Metcalfe, 2013). The Loei Fold Belt is situated in the eastern part of the eastern granite belt and traverses eastern Thailand and Laos from north to south, whereas the western part of the eastern granite belt belongs to the Sukhothai Zone (Salam et al., 2014; Khin Zaw et al., 2014). The Loei fold belt is a back arc basin formed by the eastward subduction of the Paleo-Tethys Ocean beneath the Indochina terrane (Bunopas, 1981). As a result, the Sukhothai Zone (the Sukhothai arc) was separated from the western Indochina terrane (Ueno and Hisada, 2001; Sone and Metcalfe, 2008; Sone et al., 2012). Granitic bodies in Chanthaburi and Chachoengsao provinces in the eastern
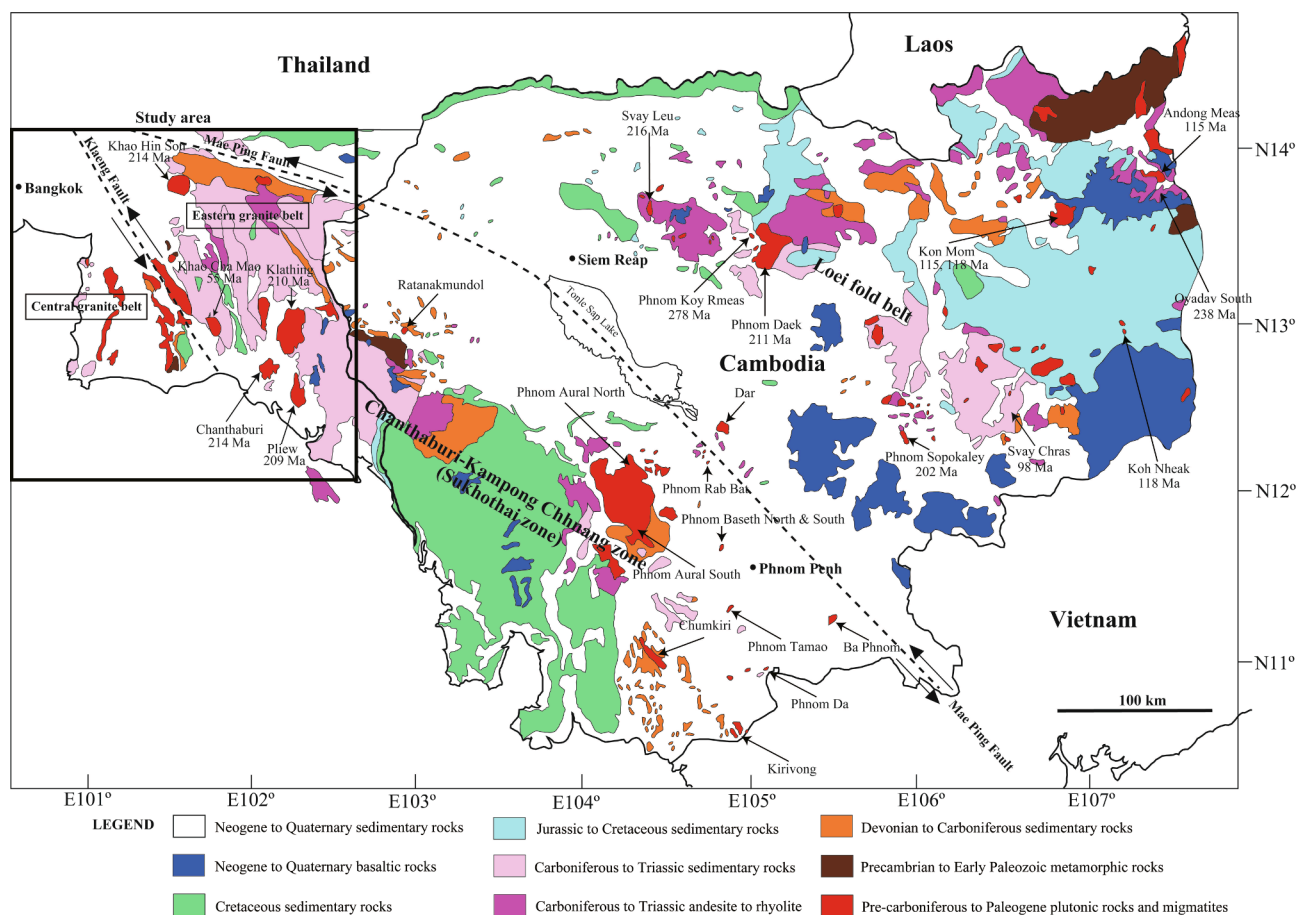

Fig. 1. Geological map of Cambodia and southeastern Thailand based on Tien et al. (1990), Mantajit and Hintong (1999) and Cheng et al. (2019).

granite belt (Figs. 1 and 2) were previously considered to belong to the Loei Fold Belt based on the metal ore deposit distribution (e.g., Nualkhao et al., 2018) or to the Sukhothai Zone based on the stratigraphy, especially occurrence of late Permian lyttoniid brachiopod (*Oldhamina*) shale (e.g., Sone et al., 2012). The granitic rock properties differ across the Mae Ping Fault (the Wang Chao Fault), which runs in the southern region of the eastern granite belt (Nualkhao et al., 2018). We had conducted a magnetic and geochemical survey of the plutonic rocks distributed in Cambodia (Cheng et al, 2019) and found that their magnetic and geochemical signatures differ across the Mae Ping Fault (48–24 Ma) (Nachtergaele et al., 2020), which is deduced to cross Cambodia from the northwest to south. With this background, we investigated the granitic bodies in Chanthaburi and Chachoengsao provinces located on the southwestern side of the Mae Ping Fault in southeastern Thailand, which is an extensional area to the northwest of southwestern Cambodia (Figs. 1 and 2). We investigated the magnetic and geochemical signatures and performed zircon U-Pb dating and Nd-Sr isotope ratio measurements for the granitic bodies in Chanthaburi and Chachoengsao provinces in order to determine whether the study area belongs to the Loei Fold Belt (Kamvong et al., 2014; Nualkhao et al., 2018) or the Sukhothai Zone (the Chanthaburi-Kampong Chhnang Zone) (Sone et al., 2012).

2. Geological setting

We investigated the granitic rocks located in Chanthaburi and Chachoengsao provinces in southeastern Thailand located on the southwestern side of the Mae Ping Fault and eastern side of the Klaeng Fault (termed the Klaeng tectonic line in Sone et al., 2012) (Figs. 1 and 2). The study was conducted on five granitic bodies: Chanthaburi, Pliew
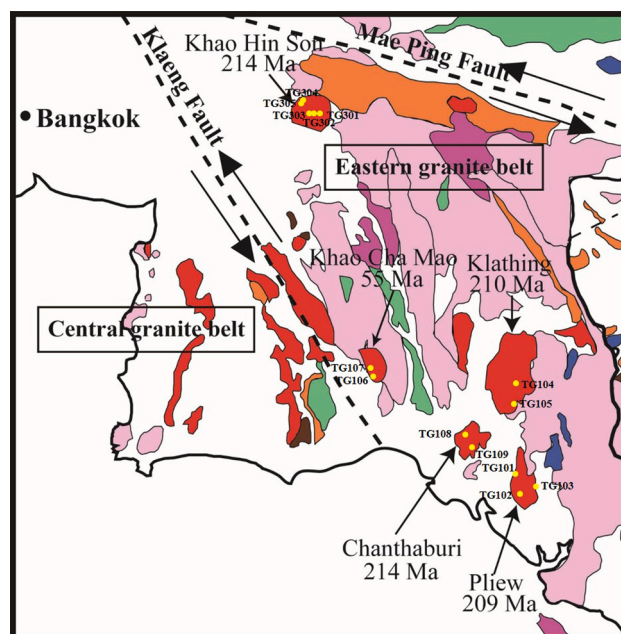

Fig. 2. Geological map showing the location of the investigated granitic bodies (Mantajit and Hintong, 1999). Sampling points are indicated by yellow circles. The legend is the same as that in Fig. 1. (For interpretation of the references to colour in this figure legend, the reader is referred to the web version of this article.)

(termed Chanthaburi in Charusiri et al., 1992), Klathing (termed Khao Soi Dao in Charusiri et al., 1992), Khao Cha Mao, and Khao Hin Son (Fig. 2). No systematic geochemical study for these granitic bodies has not been conducted previously. In addition to the granitic rocks, Carboniferous-Triassic shallow to deep marine sedimentary rocks and Quaternary alluvium are widely distributed in the study area (e.g., Sone et al., 2012), and Neogene to Quaternary intraplate basalt is also locally distributed (Figs. 1 and 2).

According to Cheng et al. (2019), the plutonic rocks in northeastern Cambodia, bordered by the Mae-Ping fault have a wide compositional range (46–72 wt% SiO_2), are of the magnetite series, mostly classified as I-type, volcanic arc-types with adakitic properties, and their source is thought to be upper mantle material. In contrast, the plutonic rocks in southwestern Cambodia are classified as granite (67–80 wt% SiO_2), mostly of the ilmenite series, I- to A-type, with non-adakitic properties and a clearly negative Eu anomaly in the rare earth element (REE) pattern (Cheng et al., 2019). Continental crust material is considered to have had a large influence on the source of the plutonic rocks in southwestern Cambodia (Cheng et al., 2019). The above characteristics suggest the plutonic rocks in northeastern Cambodia were generated in an extensional field with rising upper mantle material, whereas the plutonic rocks in southwestern Cambodia formed in a compressional field and reacted with continental crust material (Kasahara et al., 2021). Northeastern Cambodia is therefore considered to correspond to the back-arc caused by the subduction of the Paleo-Tethys Ocean beneath the Indochina terrane and is an extension of the Loei Fold Belt in Thailand, whereas southwestern Cambodia is considered to correspond to the Sukhothai Zone (Kasahara et al., 2021). The Mae Ping Fault is thus an important feature that separates northeastern Cambodia from southwestern Cambodia.

3. Material and methods

3.1. Sampling, magnetic susceptibility measurement, and sample preparation

One fresh granitic rock sample was collected at each outcrop. Magnetic susceptibilities were measured using a portable magnetic susceptibility meter (SM30, ZH Instruments, Brno, Czech Republic) at 10 points at each outcrop of the granitic bodies. A fresh and flat surface that was not covered with lichens or algae was selected for measurement.

Thin sections were prepared from the collected rock samples and observed under a transmission polarizing microscope. The collected sample was pulverized for 1 min using a rod mill made of tungsten carbide (TI-100, Heiko Seisakusho Ltd., Fukushima, Japan) for whole-rock chemical composition analysis.

3.2. Analytical methods

The pulverized samples were sent to Activation Laboratories, Ltd. (Ancaster, Canada) for whole-rock chemical composition analysis based on the "4Litho" litho-geochemistry package. Tungsten and cobalt were removed from the chemical analysis results due to contamination from the tungsten carbide used in the rod mill. In the whole-rock chemical composition analysis, the rock powder sample was fused using lithium metaborate/tetraborate and then digested using dilute nitric acid. Inductively coupled plasma atomic emission spectrometry (ICP-AES) and inductively coupled plasma mass spectrometry (ICP-MS) were used to analyze 55 elements.

We conducted Nd-Sr isotope ratio measurements at the Research Institute for Humanity and Nature in Kyoto, Japan. Approximately 0.1 g of powdered sample was dissolved using mixed solutions of nitric acid (HNO_3), hydrofluoric acid (HF), and perchloric acid ($HClO_4$) in a digestion bomb with a liner made of poly tetra fluoronitrate at 160 °C. Sr and Nd were then separated using a resin-loaded column. A multi-collector ICP-MS (NEPTUNE, Thermo Fisher Scientific Inc., MA, USA)

was used for the Sr and Nd isotope ratio measurements. Measured $^{87}Sr/^{86}Sr$ and $^{143}Nd/^{144}Nd$ isotope ratios were normalized with respect to $^{86}Sr/^{88}Sr = 0.1194$ and $^{146}Nd/^{144}Nd = 0.7219$, respectively. Repeated analyses of the standard samples NIST SRM 987 and JNdi-1 yielded an average $^{87}Sr/^{86}Sr$ value of 0.71029 ± 0.00004 (2σ) (n = 5) and $^{143}Nd/^{144}Nd$ value of 0.512099 ± 0.000018 (2σ) (n = 7), respectively. Sr and Nd isotope ratios of the samples were corrected with respect to standard values $^{87}Sr/^{86}Sr = 0.710250$ (NIST SRM 987) (Faure and Mensing, 2005) and $^{143}Nd/^{144}Nd = 0.512115$ (JNdi-1) (Tanaka et al., 2000), respectively. For more details of the Sr and Nd separation and standard samples, refer to Shin et al. (2009).

For the separation of zircon grains used for U-Pb dating, we crushed the collected samples to 250 μm or smaller, panned in water, and the residual grains were dried. After removing the magnetic minerals using a neodymium magnet, the heavy minerals were recovered using a sodium polytungstate solution with a specific gravity of approximately 2.85 g/cm³. Approximately 20 zircon grains were selected by hand-picking under a stereomicroscope. Zircon grains were embedded in Petropoxy 154 resin thinly coated on a glass slide and warmed on a hot plate at 140 °C to cure. The embedded zircon grains were then polished with #1200 and #2500 water-resistant abrasive papers followed by 3- and 0.25-μm diamond pastes to expose the center of the zircon grains. Carbon coating was performed on the glass slide in which the zircon grains were embedded. The cathodoluminescence detector (MonoCL3, Gatan, CA, USA) attached to the field emission type electron microscope (JSM-7001F, JEOL, Tokyo, Japan) installed at the Kagami Memorial Research Institute for Materials Science and Technology of Waseda University was used to take cathodoluminescence images of the zircon grains. U-Pb dating measurements were performed at the Geochemical Research Center of the Graduate School of Science at the University of Tokyo. A multi-collector ICP-MS (Nu Plasma 2, Wrexham, UK) equipped with six high-gain ion detectors was used for the measurement. An in-house laser ablation system with a Yb: KGW femtosecond laser (Carbide, Light Conversion, Lithuania) was used to ablate the zircon grains in a He atmosphere. The laser beam has 2 Hz frequency and 3 J/cm² energy. The integration time was 22 s. The size of the pits produced by laser ablation was 10–15 μm. The pre-ablation was performed over a 50 × 50 μm region. NIST SRM 610 standard glass ($^{207}Pb/^{206}Pb = 0.9096$) or NIST SRM 612 standard glass ($^{207}Pb/^{206}Pb = 0.9073$) was used for gain calibration of the high-gain ion detectors (Jochum and Brueckner, 2008). As a primary standard sample, Nancy 91,500 standard zircon ($^{206}Pb/^{238}U$ ratio: 0.17928 ± 0.00018, $^{207}Pb/^{206}Pb$: 0.07556 ± 0.00032) was used to correct the $^{206}Pb/^{238}U$ ratio (Sakata et al., 2017). GJ-1 standard zircon ($^{206}Pb/^{238}U$ age: 600.4 Ma) was used as a secondary standard sample (Jackson et al., 2004). The U–Pb isotopic analysis consists of three points on NIST SRM 610 standard glass or NIST SRM 612 standard glass, three points on Nancy 91,500 standard zircon, one point on GJ-1 standard zircon, 13 points on zircon samples, three points on NIST SRM 610 standard glass or NIST SRM 612 standard glass, and three points on Nancy 91,500 standard zircon. Refer to Kasahara et al. (2021) for more details of zircon U-Pb dating.

Wetherill diagrams were created using IsoplotR (Vermeesch, 2018) for the concordant zircon samples and the crystallization age was calculated. A zircon grain is defined as concordant if it has an error ellipse of 95% confidence (±2σ) that overlaps with the concordia curve. The concordia ages were obtained from the two-dimensional weighted means of the $^{207}Pb/^{235}U$ and $^{206}Pb/^{238}U$ ratios (Ludwig, 1998).

4. Descriptions of rock samples

Table 1 summarizes the mineral assemblages of the studied granitic rocks. Photographs of representative rock samples and their photomicrographs are shown in Fig. 3. Cathodoluminescence images of representative zircon grains used for U-Pb dating are shown in Fig. 4.

Table 1
Mineral assemblages of the collected granitic rocks.

	Sample No.	Rock type	Q	Pl	Kf	Bi	Hb	Zr	Ap	Mu	Ttn	Op	Ep	Ru	Cpx	Tour	Alla	Remarks
Pliew	TG101	Hornblende biotite granite	◎	◎	◎	○	○		–			–					–	Pl is partly altered.
	TG102	Hornblende biotite granite	○	◎	◎	○	○				△	–						Bi is altered.
	TG103	Hornblende biotite granite	○	◎	○	○	○	–	–			–						
Klathing	TG104	Hornblende biotite granite	○	○	◎	○	○	–	–			–					–	Bi and Pl are partly altered.
	TG105	Hornblende biotite granite	○	○	◎	○	○	–									–	
Khao Cha Mao	TG106	Biotite granite	◎	○	○	○		–	–		–							Pl is partly altered.
	TG107	Biotite granite	◎	○	○	○		–	–		–							Pl is altered.
Chanthaburi	TG108	Biotite granite	◎	○	◎	○		–	–		–	–	–				–	
	TG109	Biotite granite	○	○	◎	○		–	–		–	–	–			–	–	Mu is altered.
Khao Hin Son	TG301	Hornblende biotite granite	◎	◎	◎	○	○	–	–		△							Pl is partly altered.
	TG302	Biotite granite	◎	○	◎	○		–	–		△	–						Pl is partly altered.
	TG303	Hornblende biotite granite	◎	◎	◎	○	△	–	–		△	–						Pl is altered.
	TG304	Biotite granite	◎	◎	◎	○		–	–			–						Pl is partly altered. Bi is partly distorted.
	TG305	Biotite granite	◎	◎	◎	○		–	–			–						Kf is partly altered. Bi is partly distorted and altered.

Modal proportions: ◎: > 30 vol%, ○: 30–10 vol%, △: 10–2 vol%, and –: < 2 vol%.
Abbreviations: Q, Quartz; Pl, Plagioclase; Kf, Potassium feldspar; Bi, Biotite; Hb, Hornblende; Zr, Zircon; Ap, Apatite; Mu, Muscovite; Ttn,Titanite; Op, Opaque minerals; Ep, Epidote; Ru, Rutile; Cpx, Clinopyroxene; Tour, Tourmaline; Alla, Allanite.

4.1. Pliew granitic rock

The Pliew granitic rock is a medium-grained hornblende-biotite granite and is rich in euhedral plagioclase, anhedral potassium feldspar and quartz. All collected samples contain biotite and hornblende, in addition to apatite, zircon, allanite, and opaque minerals as accessory minerals. Biotite and plagioclase were partially altered into chlorite and clay minerals, respectively. Zircon grains show columnar shapes with lengths of 150–400 μm. Several mineral inclusions are found. Zircon grains show a clear zonal structure in the cathodoluminescence images (Fig. 4).

4.2. Klathing granitic rock

The Klathing granitic body is also called the Khao Soi Dao Tai granitic body (Charusiri et al., 1992). This granitic rock is a coarse-grained hornblende-biotite granite, and is composed mainly of sub-hedral to anhedral potassium feldspar with a perthite texture, euhedral plagioclase and anhedral quartz. Biotite and hornblende are found in all samples, in addition to zircon, allanite, opaque minerals, and apatite as accessory minerals. Plagioclase is partially altered into clay minerals. Most zircon grains show spindle shapes and many have lengths of 90–150 μm. A residual core and clear zonal structure are seen in the cathodoluminescence images (Fig. 4).

4.3. Chanthaburi granitic rock

The Chanthaburi granitic rock is a coarse-grained biotite granite, and is composed mainly of potassium feldspar with a microcline texture, quartz and plagioclase. Biotite can be seen, but hornblende is absent. Zircon, allanite, epidote, and opaque minerals are commonly recognized as accessory minerals. Additionally, tourmaline, muscovite, and apatite are rarely found. Zircon has a long columnar crystal form with lengths of 120–330 μm, but many crystals show irregular shapes. A clear zonal structure can be seen in the cathodoluminescence images (Fig. 4).

4.4. Khao Hin Son granitic rock

The Khao Hin Son granitic rock is a medium-grained biotite granite to hornblende-biotite granite, and contains approximately equal amounts of quartz, plagioclase, and potassium feldspar with a microcline texture. Biotite is commonly observed. Some samples contain hornblende and others do not. Zircon, apatite, titanite, epidote, and opaque minerals are recognized as accessory minerals. Plagioclase is extensively altered. Zircon grains have long columnar shapes with lengths of 100–230 μm. Mineral inclusions are commonly observed in zircon. A residual core is seen in the cathodoluminescence images with a surrounding zonal structure (Fig. 4).
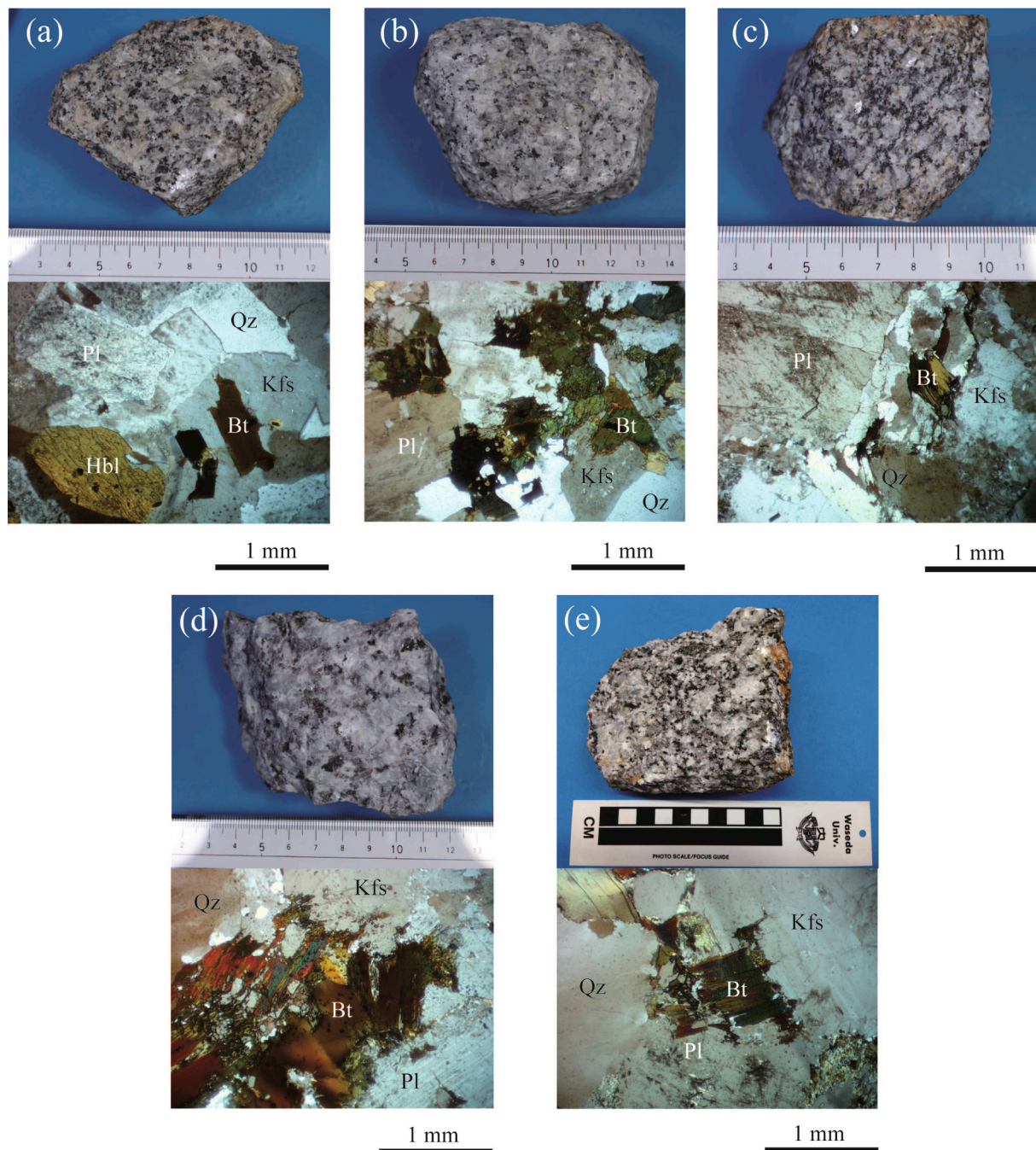
4.5. Khao Cha Mao granitic rock

The Khao Cha Mao granitic rock is a biotite granite with a shear texture. This rock is composed mainly of poly-crystalline quartz, plagioclase and potassium feldspar. Biotite is observed, but hornblende is absent. Zircon, apatite, and muscovite are observed as accessory minerals. Plagioclase and biotite alteration are observed. Zircon crystals have long columnar shapes with lengths of 50–130 μm. A clear zonal structure can be seen in the cathodoluminescence images (Fig. 4).

5. Results

5.1. Magnetic susceptibility

The five surveyed granite bodies show low magnetic susceptibilities

Fig. 3. Photographs (above) of the granitic rock samples taken from southeastern Thailand and photomicrographs (below) of their thin sections under cross-polarized light. Granitic rocks from (a) Pliew (TG103), (b) Klathing (TG105), (c) Khao Cha Mao (TG107), (d) Chanthaburi (TG108), and (e) Khao Hin Son (TG302). Abbreviations: Pl, plagioclase; Qz, quartz; Kfs, potassium feldspar; Bt, biotite; and Hbl, hornblende.

of 0.01–0.2 × 10^{-3}SI units (Fig. 5). The granites are low in opaque minerals, reflecting their low magnetic susceptibility (Table 1). Igneous rocks with magnetic susceptibilities higher and lower than 3 × 10^{-3}SI units belong to the magnetite and ilmenite series, respectively. Thus, the measured magnetic susceptibilities suggest that all five of the granite bodies in the study area belong to the ilmenite series (Ishihara, 1981).

5.2. Geochemical characteristics

5.2.1. Classification

Table 2 shows the results of the whole-rock chemical composition analysis of the collected samples. The SiO_2 content of the samples ranges from 69 to 80 wt%. Based on the total alkali versus silica diagram

(Fig. 6a), all five surveyed granitic rocks are classified as granite (Cox et al., 1979; Wilson, 1989).

Based on the $Al_2O_3/(Na_2O + K_2O)$ versus $Al_2O_3/(CaO + Na_2O + K_2O)$ (A/NK versus A/CNK) diagram (Fig. 6b) (Middlemost, 1994), all of the granites are classified as I-type. Based on the I&S-type and A-type classification diagram (Whalen et al., 1987) (Fig. 6c), the Chanthaburi granite is classified as A-type instead of I&S type, and the other granites plot near the boundary between I&S-type and A-type. As a result, the investigated granites are predominantly I-type with the exception of the Chanthaburi granite (A-type).

Furthermore, based on the tectonic setting classification diagram (Fig. 6d) (Pearce et al., 1994), most of the investigated granites are classified as *syn*-collision granites, and the remaining are classified as
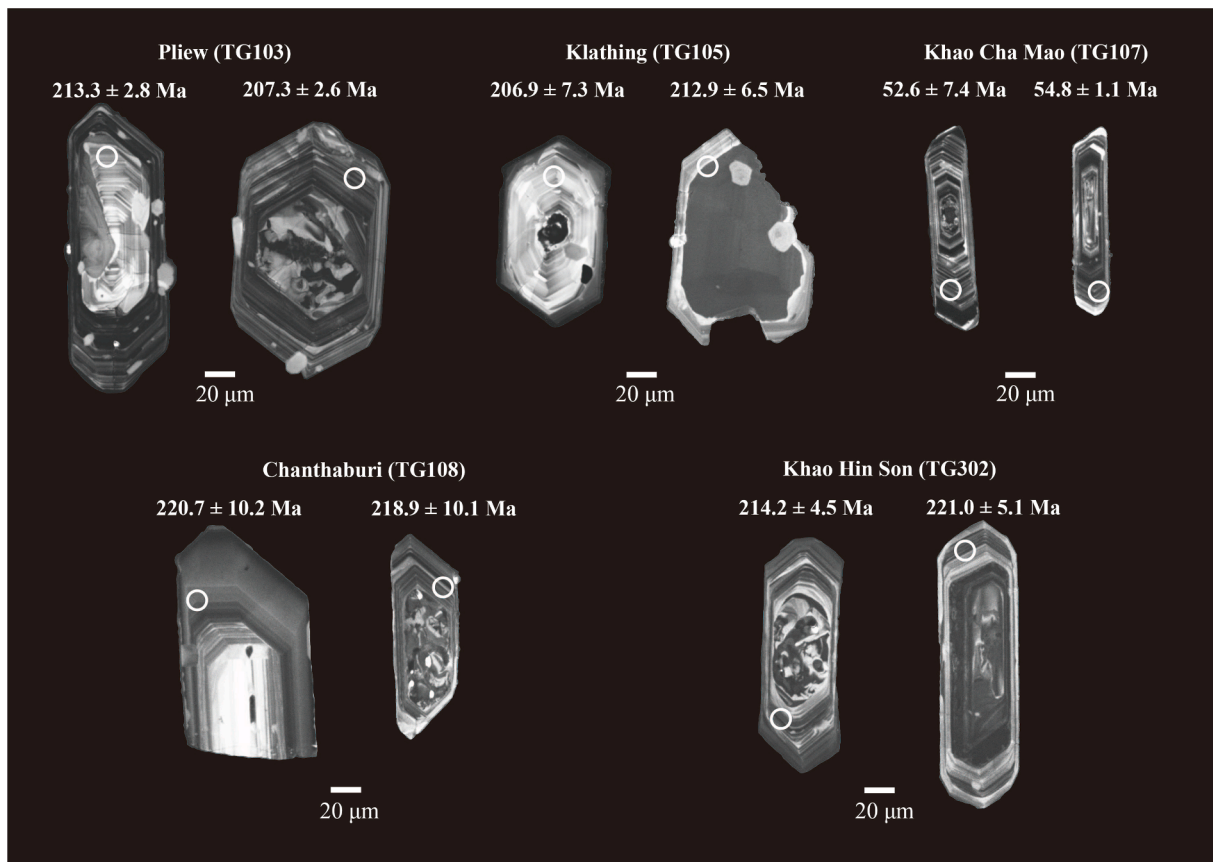
Fig. 4. Representative cathodoluminescence images of zircon grains from the granitic rock samples for U-Pb dating. Circles show the positions of the analyzed points. The U-Pb ages of each zircon grain are (^{206}Pb/^{238}U) ages.
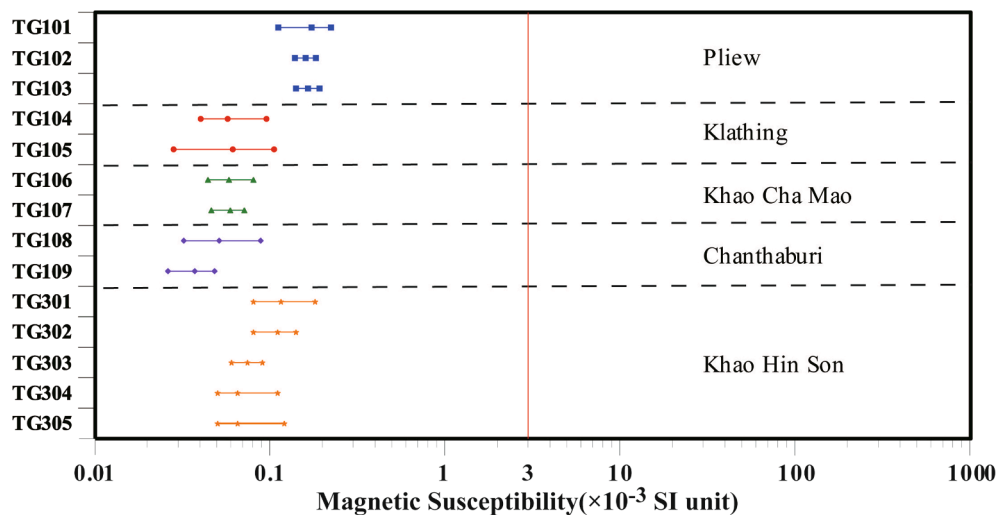

Fig. 5. Magnetic susceptibilities of the granites in the study area. Maximum, average, and minimum values are shown.

volcanic arc granites or within-plate granites.

5.2.2. Major components, trace elements, and REE patterns

The Harker diagrams of major components and incompatible elements Rb, Y, Sn, U, Pb, and Th are shown in Figs. 7 and 8, respectively.

Al_2O_3, $Fe_2O_3(T)$, MnO, MgO, CaO, TiO_2 and P_2O_5 decrease with increasing SiO_2 (Fig. 7). On the other side, K_2O increases with increasing SiO_2. Na_2O seems to be nearly constant with increasing SiO_2. The average contents of incompatible elements Rb, Y, Sn, U, Pb, and Th are

224, 45, 9.6, 7.6, 33, and 33 ppm, respectively. In contrast, those in the continental crust are 49, 19, 1.7, 1.3, 11, and 5.6 ppm, respectively (Rudnick and Gao, 2005). The investigated granites are rich in these elements compared with the continental crust. The Rb, Y, U, Pb and Th increase with increasing SiO_2 (Fig. 8). On the other hand, Sn decreases with increasing SiO_2. According to Uchida et al. (2017) and Cheng et al. (2019), this tendency is also observed for granitic rocks in Japan and Cambodia: Sn is saturated when SiO_2 reaches approximately 70–75 wt% and then decreases as the crystal differentiation progresses further.

Table 2
Whole-rock chemical composition of the granitic rock samples.

| Locality	Pliew			Klathing		Khao Cha Mao		Chanthaburi		Khao Hin Son				
Sample No.	TG101	TG102	TG103	TG104	TG105	TG106	TG107	TG108	TG109	TG301	TG302	TG303	TG304	TG305
SiO$_2$	70.10	69.73	69.25	74.94	74.03	74.60	74.80	79.73	78.49	71.22	71.82	71.99	73.98	74.70
Al$_2$O$_3$	13.49	14.05	14.65	13.52	13.70	14.25	13.62	10.34	11.81	12.71	13.62	13.35	13.98	13.91
Fe$_2$O$_3$(T)	4.13	4.26	4.42	1.75	1.61	1.39	1.94	2.16	1.25	4.04	3.29	2.50	1.65	2.12
MnO	0.064	0.089	0.067	0.028	0.025	0.032	0.061	0.014	0.013	0.070	0.052	0.066	0.033	0.043
MgO	0.70	0.72	0.72	0.17	0.15	0.22	0.30	0.14	0.04	0.65	0.51	0.42	0.40	0.47
CaO	2.26	2.67	2.56	1.13	1.14	1.34	1.49	1.17	0.62	2.63	2.18	2.00	1.94	2.08
Na$_2$O	3.14	4.33	3.66	4.16	4.19	3.10	3.32	2.13	2.52	3.16	3.27	3.44	3.40	3.66
K$_2$O	4.43	3.59	4.08	4.71	4.12	5.49	4.61	4.33	5.23	3.12	4.07	3.76	3.98	3.02
TiO$_2$	0.494	0.565	0.529	0.164	0.133	0.168	0.230	0.240	0.095	0.597	0.429	0.276	0.166	0.209
P$_2$O$_5$	0.10	0.11	0.11	0.02	0.02	0.03	0.05	0.02	< 0.01	0.13	0.09	0.08	0.05	0.03
LOI	0.62	0.81	0.79	0.37	0.70	0.38	0.55	0.37	0.73	0.85	0.75	0.78	0.70	0.69
Total	99.54	100.90	100.80	101.00	99.80	101.00	101.00	100.60	100.80	99.18	100.10	98.65	100.30	100.90
Sc	9	9	11	6	5	4	6	4	3	9	7	6	4	5
Be	2	6	4	3	3	7	4	2	3	4	4	4	2	2
V	38	39	40	9	9	9	15	6	< 5	25	18	13	12	11
Ba	347	289	412	341	390	413	380	52	22	152	267	186	584	392
Sr	119	148	141	47	39	136	116	30	13	97	109	82	187	184
Y	47	37	62	38	35	18	25	46	99	81	37	58	15	26
Zr	217	250	274	134	165	140	184	292	127	208	219	155	80	97
Cr	< 20	< 20	< 20	< 20	< 20	< 20	< 20	< 20	< 20	< 20	< 20	< 20	< 20	< 20
Ni	< 20	< 20	< 20	< 20	< 20	< 20	< 20	< 20	< 20	< 20	< 20	< 20	< 20	< 20
Cu	20	10	10	< 10	< 10	< 10	< 10	20	< 10	10	< 10	< 10	< 10	< 10
Zn	70	70	70	40	40	40	70	60	110	80	60	60	40	50
Ga	19	21	22	20	20	19	21	18	20	21	21	20	15	17
Ge	2	3	3	2	2	2	2	2	2	2	2	2	1	1
As	11	10	7	< 5	< 5	< 5	< 5	< 5	< 5	< 5	< 5	< 5	< 5	< 5
Rb	217	174	212	197	166	283	292	257	371	228	241	230	138	130
Nb	4	7	6	6	6	11	22	10	11	17	10	9	4	5
Mo	< 2	< 2	< 2	< 2	< 2	< 2	< 2	3	< 2	< 2	< 2	< 2	< 2	< 2
Ag	0.5	1.1	0.8	< 0.5	0.7	< 0.5	0.7	1.0	< 0.5	1.1	1.1	0.8	< 0.5	0.5
In	< 0.2	< 0.2	< 0.2	< 0.2	< 0.2	< 0.2	< 0.2	< 0.2	< 0.2	< 0.2	< 0.2	< 0.2	< 0.2	< 0.2
Sn	19	27	10	3	5	11	7	5	6	13	10	10	4	5
Sb	< 0.5	< 0.5	< 0.5	< 0.5	< 0.5	< 0.5	< 0.5	< 0.5	< 0.5	0.6	0.6	0.7	< 0.5	< 0.5
Cs	33.0	32.1	22.6	9.4	13.3	31.3	21.7	33.1	16.8	41.8	37.0	36.9	9.6	14.6
La	34.2	35.0	41.4	26.4	25.6	43.9	54.1	81.4	39.9	48.9	38.9	45.4	39.9	38.9
Ce	66.8	66.1	82.2	53.9	51.3	83.7	101.0	174	81.8	100	78.1	81.0	77.3	74.8
Pr	8.01	8.04	10.1	6.88	6.45	9.57	11.6	22.4	11.9	12.9	9.54	11.00	8.78	8.66
Nd	30.4	30.3	38.2	26.9	24.7	33.4	41.5	83.3	49.2	51.6	35.6	42.7	32.6	30.6
Sm	6.7	6.6	8.6	6.5	5.4	6.3	8.2	17.4	15.0	13.4	7.4	9.9	5.5	5.5
Eu	0.95	1.13	1.09	0.44	0.47	0.52	0.48	0.35	0.20	0.96	0.93	0.99	0.63	0.57
Gd	7.1	6.5	9.1	6.5	5.4	4.9	6.7	13.0	17.6	13.5	6.8	10.7	3.8	4.4
Tb	1.2	1.1	1.5	1.2	1.0	0.6	1.0	1.9	3.1	2.3	1.1	1.7	0.5	0.7
Dy	7.4	6.8	9.6	7.0	5.9	3.3	5.0	10.0	18.3	15.4	6.5	10.8	2.6	4.2
Ho	1.5	1.4	1.9	1.4	1.2	0.6	0.9	1.8	3.6	3.2	1.4	2.2	0.5	0.9
Er	4.4	4.1	5.6	4.2	3.7	1.5	2.5	4.9	9.9	9.3	4.2	6.6	1.4	2.7
Tm	0.69	0.66	0.89	0.65	0.58	0.23	0.36	0.72	1.39	1.39	0.63	0.98	0.23	0.39
Yb	4.7	4.3	6.2	4.0	3.9	1.4	2.3	4.4	8.1	8.4	4.0	6.6	1.4	2.5
Lu	0.73	0.7	1.01	0.69	0.64	0.22	0.38	0.68	1.23	1.2	0.62	1.03	0.22	0.37
Hf	5.2	6.4	6.7	4.3	5.1	4.0	5.6	8.7	4.9	6.8	7.0	5.3	2.6	3.4
Ta	1	1.2	1.3	1.1	1.2	2.3	2.4	1.2	0.9	4.4	1.6	1.8	0.8	1.4
Tl	1.2	0.2	1.2	0.3	0.1	1.7	1.1	0.9	1.5	1.2	1.3	1.3	0.8	0.8
Pb	27	26	27	26	25	42	42	34	53	31	34	35	28	27
Bi	0.5	< 0.4	< 0.4	< 0.4	< 0.4	1.3	< 0.4	< 0.4	2.2	0.8	0.4	1.5	0.5	4.8
Th	24.3	20.5	28.1	14.6	18.4	33.7	50.7	68.4	80.2	34.6	23.7	25.4	19.1	21.3
U	6.0	5.1	8.9	4.0	5.2	9.2	12.5	7.3	16.8	9.3	6.2	7.1	3.0	5.8

The primitive mantle-normalized multi-element patterns of the studied granites are shown in Fig. 9a (McDonough and Sun, 1995). For comparison, the primitive mantle-normalized multi-element patterns for the granitic rocks in southwestern Cambodia are also shown in Fig. S1 of the Supplementary material. All investigated granites show similar patterns, showing distinct depletion in Ba, Ta, Nb, Sr, P, and Ti.

The chondrite-normalized REE patterns of the studied granites are also shown in Fig. 9b (McDonough and Sun, 1995). All granites are rich in light REEs and have lower heavy REEs comparing to light REEs. A distinct negative Eu anomaly is also observed. In particular, the Chanthaburi granite, which is rich in SiO$_2$, shows a larger negative Eu anomaly (Eu/Eu* = 0.012–0.023) than the other granites (Eu/Eu* = 0.064–0.173).

5.3. Zircon U-Pb geochronology

Zircon U-Pb dating was performed on samples TG103, TG105, TG107, TG108, and TG302, which were selected from the Pliew, Klathing, Chanthaburi, Khao Cha Mao, and Khao Hin Son granite bodies, respectively. The results for each zircon grain are summarized in Table S1 of the Supplementary material.

The results show a relatively narrow age range of 208–214 Ma, which indicates that these granite bodies formed in the Late Triassic (Fig. 10). The only exception is the Khao Cha Mao granite body, which has a zircon U-Pb age of 55 Ma, indicating formation in the Paleogene (Fig. 10).
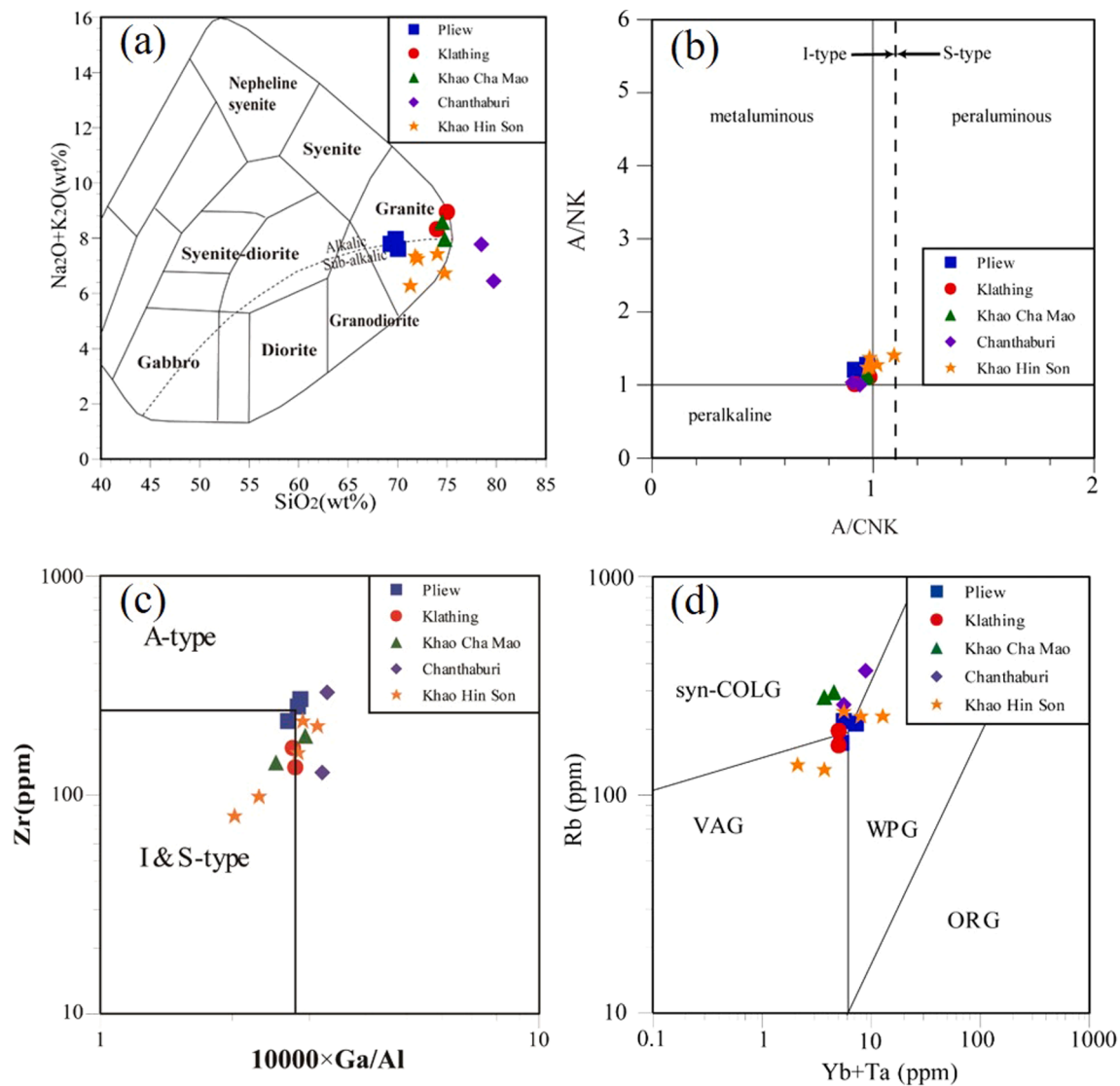
Fig. 6. (a) Classification of the granitic rock samples based on a total alkali versus silica diagram (Cox et al., 1979; Wilson, 1989), (b) $Al_2O_3/(Na_2O + K_2O)$ versus $Al_2O_3/(CaO + Na_2O + K_2O)$ (A/NK versus A/CNK), showing the classification of I- and S-types (Middlemost, 1994), (c) Zr versus Ga/Al $\times$ 10,000 for the classification of I&S- and A-types (Whalen et al., 1987) and (d) tectonic setting classification diagram of the granitic rocks (Pearce et al., 1984).

5.4. Nd-Sr isotope ratios

Table 3 lists the Nd and Sr isotope ratios ($^{143}Nd/^{144}Nd$ and $^{87}Sr/^{86}Sr$) for each sample and the initial values of the Nd and Sr isotope ratios (($^{143}Nd/^{144}Nd)_i$ and ($^{87}Sr/^{86}Sr)_i$), which were obtained using the ages yielded by the zircon U-Pb dating for each granite body. Fig. 11 shows a ($^{87}Sr/^{86}Sr)_i$ versus ($^{143}Nd/^{144}Nd)_i$ diagram. The ($^{143}Nd/^{144}Nd)_i$ values of all granite samples show small variations (0.51225–0.51245), whereas the ($^{87}Sr/^{86}Sr)_i$ values show a wide range (0.70078–0.72165). The exception is the Chanthaburi granite body, which yields high ($^{87}Sr/^{86}Sr)_i$ values of 0.71121–0.72165. This suggests that the Chanthaburi granite body has taken up more continental crust material. Some granite samples plot around EM1 (enriched mantle 1), but many granite samples have higher ($^{87}Sr/^{86}Sr)_i$ values.

6. Discussion

6.1. Geochemical and magnetic signatures

This investigation conducted on the granitic bodies in Chanthaburi and Chachoengsao provinces in southeastern Thailand, which is in the extensional area of southwestern Cambodia to Thailand (Fig. 1). The survey was conducted on five granitic bodies, Chanthaburi, Pliew, Klathing, Khao Cha Mao, and Khao Hin Son, located on the southwestern side of the Mae Ping Fault and eastern side of the Klaeng Fault (Figs. 1 and 2). In terms of geochemical composition, the studied granitic rocks can be classified as I- to A-type granites. The magnetic susceptibility of all five granite bodies is very low, $0.01–0.2 \times 10^{-3}$ SI units, and they are classified as ilmenite series (Ishihara, 1981), which indicates that they formed under relatively reducing conditions. Eu is unique among REEs in having a reduced Eu^{2+} state. Eu^{2+} substitutes preferentially for Ca^{2+} in plagioclase. A negative Eu anomaly observed in the REE patterns
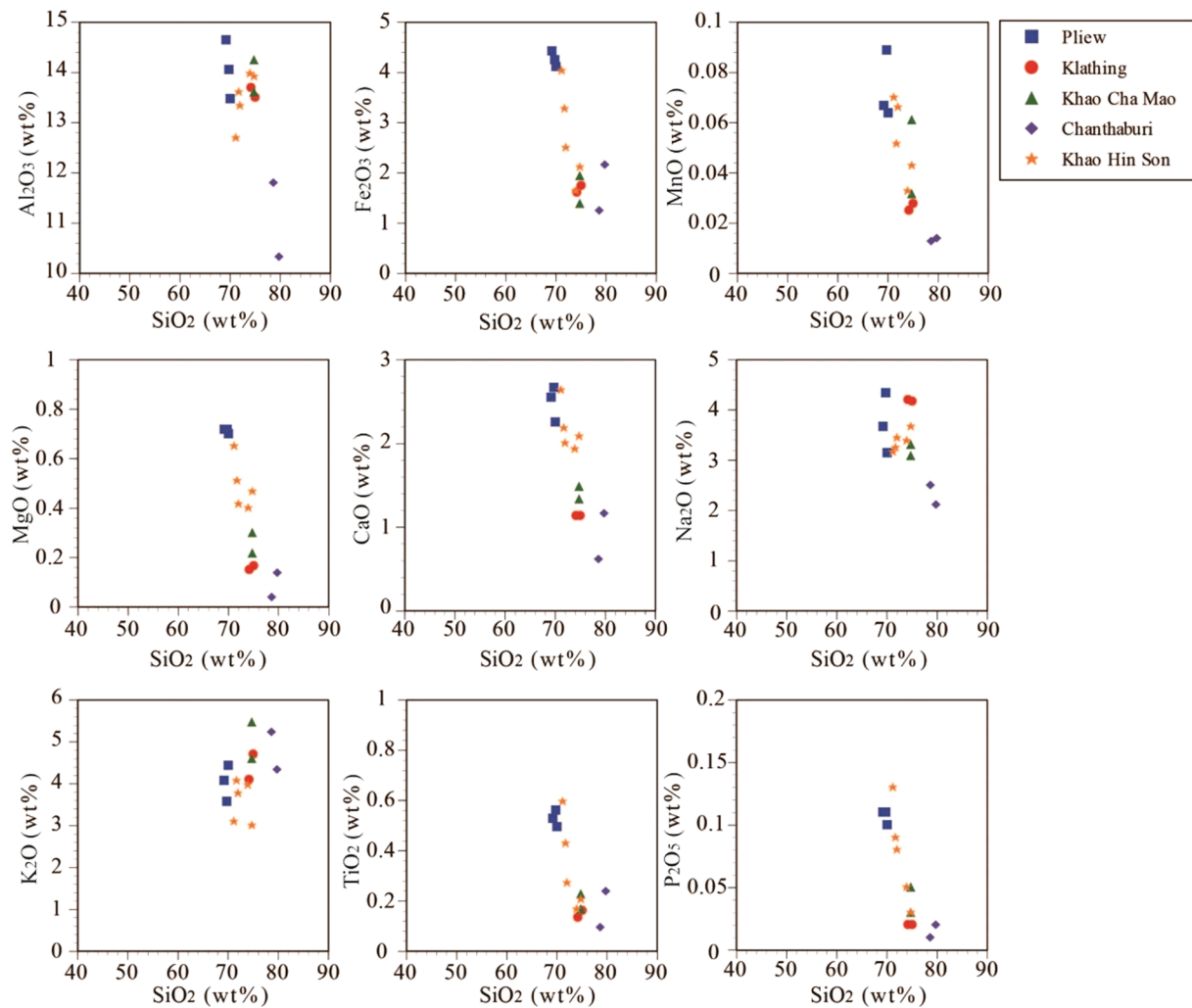
Fig. 7. Harker diagrams of major components for the collected granite samples.

supports the conclusion that the investigated granitic rocks formed under relatively reducing conditions. Because incompatible elements such as Rb, Y, Sn, U, Pb, and Th, tend to concentrate in magma as crystal differentiation progresses (Fig. 7), the investigated granites are considered to have undergone advanced crystal differentiation and/or assimilation of continental crust material. The above-mentioned geochemical and magnetic signatures of the granites in southeastern Thailand are very similar to those in southwestern Cambodia (Cheng et al., 2019).

6.2. Nd-Sr radiogenic isotopic signatures

The initial Nd isotope ratios at the time when granite bodies crystallized are almost the same in all granite bodies (0.51225–0.51245), but the initial Sr isotope ratios show a wider range of values (0.70078–0.72165). In particular, the Chanthaburi granite body shows high Sr isotope ratios (0.71121–0.72165). This indicates that continental crust material considerably contributed to the source material of the granite bodies including the Khao Cha Mao granite body (DePaolo and Wasserburg, 1979), which is consistent with the formation of the granites in a reducing environment owing to the presence of carbon in the sedimentary rocks constituting the continental crust. Reflecting this,

the Chanthaburi granite body shows a marked negative Eu anomaly in the REE pattern. Enrichments in incompatible elements such as U and Th on primitive mantle–normalized multi-element patterns (Fig. 8) support this conclusion. In addition, the depletion of Nb in the primitive mantle-normalized multi-element patterns is a characteristic of igneous rocks formed in subduction settings or inherited from continental crustal material (Azadbakht et al., 2019).

6.3. Tectonic setting

Nualkhao et al. (2018) studied the granitic rocks in the Loei Fold Belt in Thailand, including those in the study area. The geochemical signatures of the granites in the study area located on the southern side of the Mae Ping Fault and eastern side of the Klaeng Fault are similar to those of the granites in southwestern Cambodia located on the southwestern side of the Mae Ping Fault (Cheng et al., 2019). In contrast, the geochemical and magnetic signatures of the granitic rocks on the northern side of the Mae Ping Fault are similar to those of the granitic rocks in northeastern Cambodia located on the northeastern side of the Mae Ping Fault (Cheng et al., 2019). This result supports the conclusion of Sone et al. (2012) that the study area can be considered as an
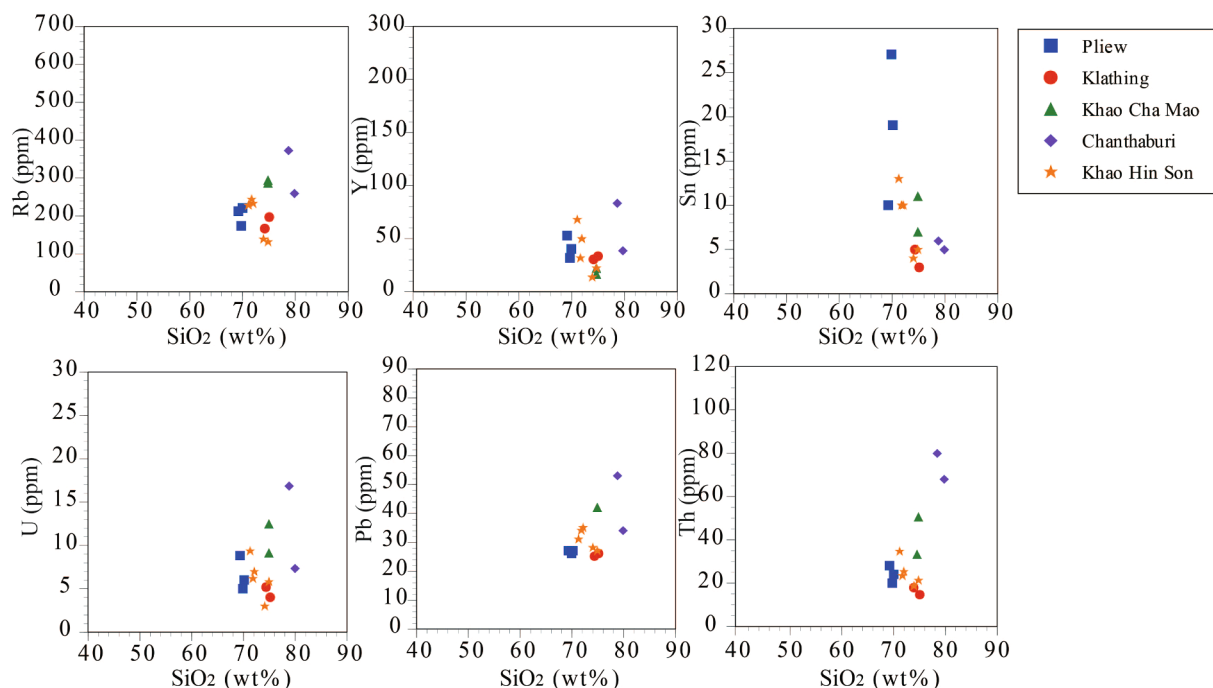
Fig. 8. Harker diagrams of incompatible elements, Rb, Y, Sn, U, Pb, and Th for the collected granite samples.

extensional area of southwestern Cambodia to Thailand, that is, the Chanthaburi-Kampong Chhnang Zone, but not the Loei Fold Belt (Fig. 12). The Chanthaburi-Kampong Chhnang zone can be correlated to the Sukhothai zone (Sone et al., 2012).

6.4. Timing of regional magmatism

The Chanthaburi, Pliew, Klathing, and Khao Hin Son granite bodies show almost the same zircon U-Pb ages of 208–214 Ma (the Late Triassic). The $^{40}Ar/^{39}Ar$ dating of the Pliew granite body by Charusiri et al. (1992), yielded 199.6–203.7 Ma. Veeravinantanakul et al. (2021) conducted zircon U-Pb dating for the Pliew granitic body, and obtained an age of 201.7 Ma. These granitic bodies intruded into Devonian to Triassic sedimentary rocks (Tien et al., 1990; Mantajit and Hintong, 1999). According to Sone and Metcalfe (2008), Metcalfe (2013), Morley et al. (2013), Khin Zaw et al. (2014), Wang et al. (2016) and Shi et al. (2021), the formation ages for the four granite bodies of 200–214 Ma almost correspond to the collision time of the Sibumasu terrane to the western Indochina terrane. This result is consistent with the fact that most granite bodies are classified as *syn*-collision granites as shown in the tectonic setting diagram in Fig. 6d (Pearce et al., 1984).

On the other hand, the Khao Cha Mao granite body indicates a zircon U-Pb age of 55 Ma (the Paleogene), which is much younger than the other four granite bodies. Zircon Pb-U dating conducted for the Khao Cha Mao granite body by Veeravinantanakul et al. (2021) yielded 43.3–59.7 Ma. The Nong Yai gneiss is located approximately 30 km northwest of the Khao Cha Mao granite body along the Klaeng Fault, and migmatite and leucogranite intrusions also occur along the Klaeng Fault. Zircon U-Pb dating of these rocks was performed by Kanjanapayont et al. (2013), yielding young ages of 67–78 Ma. The young age (43–63 Ma) for the Khao Cha Mao granite body is thus likely related to the collision of the Indian continent with the Eurasian continent (around 45 Ma)

(Metcalfe, 2011, 2013). It is therefore speculated that the Khao Cha Mao granite body formed along the Klaeng Fault in connection with the collision of the Indian continent with the Eurasian continent (Kanjana-payont et al., 2013; Veeravinantanakul et al., 2021).

Granitic rocks with the young ages of 58–118 Ma, which formed by the Andean-type magmatism, occur in the Dalat–Kratie Fold Belt extending from southern Cambodia (Cheng et al., 2019; Kasahara et al., 2021) to southern Vietnam (Thuy et al., 2004). These granitic rocks likely formed by the subduction of the Izanagi Plate (the Paleo-Pacific Ocean) beneath the South China–Indochina composite terrane. However, the Khao Cha Mao granite body is located far from the subduction zone of the Izanagi Plate. The Khao Cha Mao granite body is therefore unlikely to have formed in connection with the subduction of the Izanagi Plate beneath the South China–Indochina composite terrane (e.g., Thuy et al., 2004).

7. Conclusions

We investigated the Chanthaburi, Pliew, Klathing, Khao Cha Mao, and Khao Hin Son granitic bodies in Chanthaburi and Chachoengsao provinces in southeastern Thailand, which is an extensional area of southwestern Cambodia to Thailand, and located on the southwestern side of the Mae Ping Fault and eastern side of the Klaeng Fault. The geochemical signatures showed that these granitic rocks are classified as I- to A-type granites. The granites are of the ilmenite series and show distinct negative Eu anomalies, indicating that they formed under reducing conditions. Judging from the high initial Sr isotope ratios, continental crust material is inferred to have had a strong influence on the granite source material. The zircon U-Pb age is 208–214 Ma (the Late Triassic) for the Chanthaburi, Pliew, Klathing, and Khao Hin Son granite bodies. This period corresponds to the collision time between the Sibumasu and Indochina terranes. In contrast, the Khao Cha Mao granite
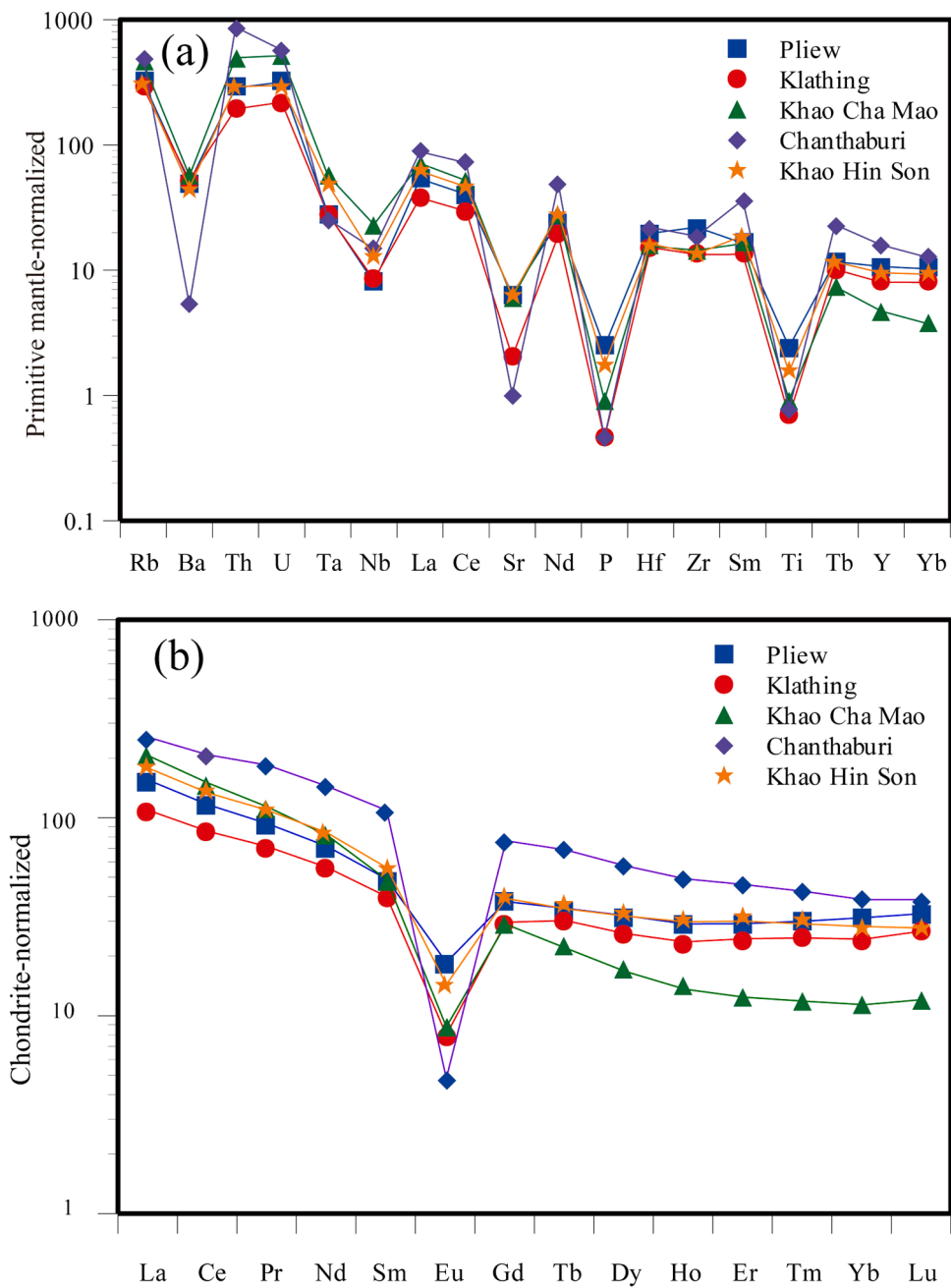
Fig. 9. (a) Primitive mantle–normalized multi-element patterns for the average chemical composition of each granite, and (b) chondrite-normalized REE patterns for the average chemical composition of each granite. The chondrite composition was taken from McDonough and Sun (1995).
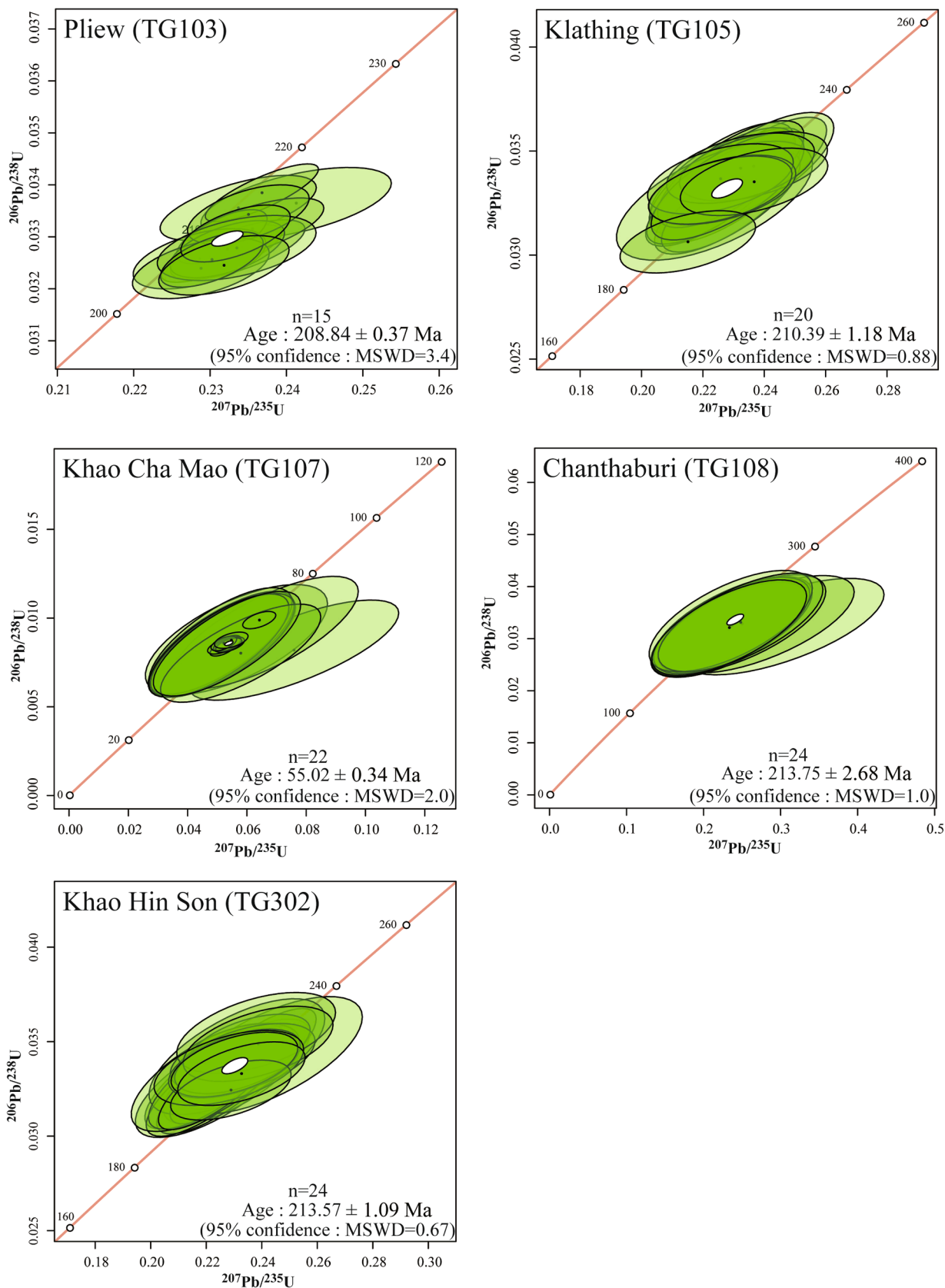
Fig. 10. Wetherill diagrams created using IsoplotR (Vermeesch, 2018) for concordant zircon grains of the granite samples. Abbreviation: MSWD, mean square weighted deviation.

Table 3
Results of Sr and Nd isotope ratio analyses.

Location	Sample No.	Zircon U-Pb age (Ma)	n	MSWD	$^{87}Sr/^{86}Sr$	$\pm 1\sigma$	$^{87}Rb/^{86}Sr$	$(^{87}Sr/^{86}Sr)_i$	$^{143}Nd/^{144}Nd$	$\pm 1\sigma$	$^{147}Sm/^{144}Nd$	$(^{143}Nd/^{144}Nd)_i$
Pliew	TG-101				0.721449	0.000008	5.15348	0.706143	0.512605	0.000005	0.138997	0.512415
	TG-102				0.716250	0.000010	3.32088	0.706388	0.512605	0.000004	0.137374	0.512417
	TG-103	208.84 ± 0.37 Ma	15	3.4	0.718013	0.000009	4.24773	0.705397	0.512643	0.000004	0.141985	0.512449
Klathing	TG-104				0.740578	0.000008	11.86789	0.705069	0.512636	0.000005	0.152394	0.512426
	TG-105	210.39 ± 1.18 Ma	20	0.88	0.746394	0.000004	12.05905	0.710315	0.512634	0.000004	0.137881	0.512444
Khao Cha Mao	TG-106				0.712084	0.000008	5.87536	0.707492	0.512437	0.000004	0.118955	0.512394
	TG-107	55.02 ± 0.34 Ma	22	2.0	0.713503	0.000009	7.10841	0.707947	0.512436	0.000004	0.124610	0.512391
Chanthaburi	TG-108	213.75 ± 2.68 Ma	24	1.0	0.785267	0.000009	24.36243	0.711208	0.512444	0.000004	0.131732	0.512260
	TG-109				0.972894	0.000009	82.64992	0.721650	0.512518	0.000005	0.192274	0.512249
Khao Hin Son	TG301				0.720958	0.000009	6.64247	0.700783	0.512556	0.000007	0.163778	0.512327
	TG302	213.57 ± 1.09 Ma	24	0.67	0.723846	0.000010	6.25001	0.704863	0.512471	0.000005	0.131091	0.512288
	TG303				0.729223	0.000009	7.93294	0.705128	0.512496	0.000005	0.146218	0.512292
	TG304				0.711093	0.000011	2.08344	0.704765	0.512474	0.000004	0.106399	0.512325
	TG305				0.712430	0.000009	1.99493	0.706371	0.512499	0.000005	0.113353	0.512340
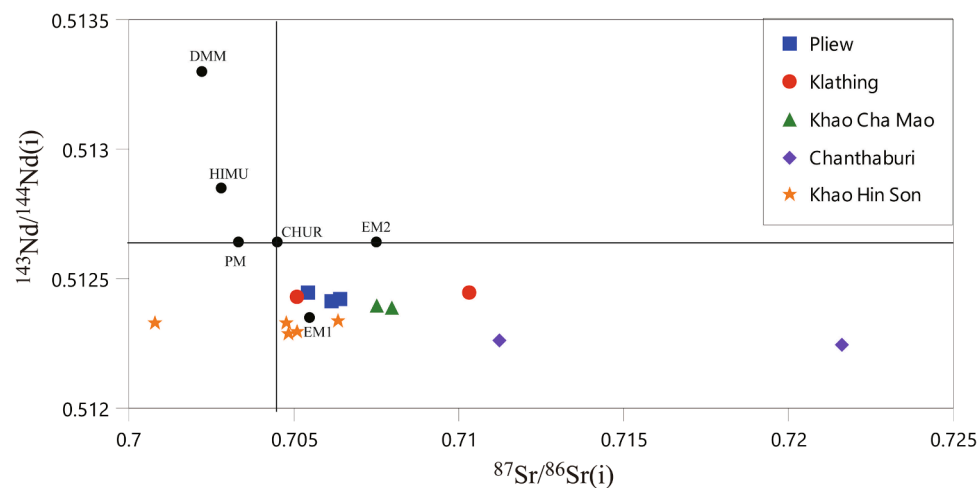
Fig. 11. $(^{87}Sr/^{86}Sr)_i$ versus $(^{143}Nd/^{144}Nd)_i$ of the studied granite samples. Abbreviations: CHUR, chondritic uniform reservoir; DMM, depleted MORB mantle; EM1, enriched mantle 1; EM2, enriched mantle 2; HIMU, high μ; and PM, primitive mantle. The data for CHUR, DMM, EM1, EM2, HIMU, and PM are from Faure and Mensing (2005) and Schaefer (2016).
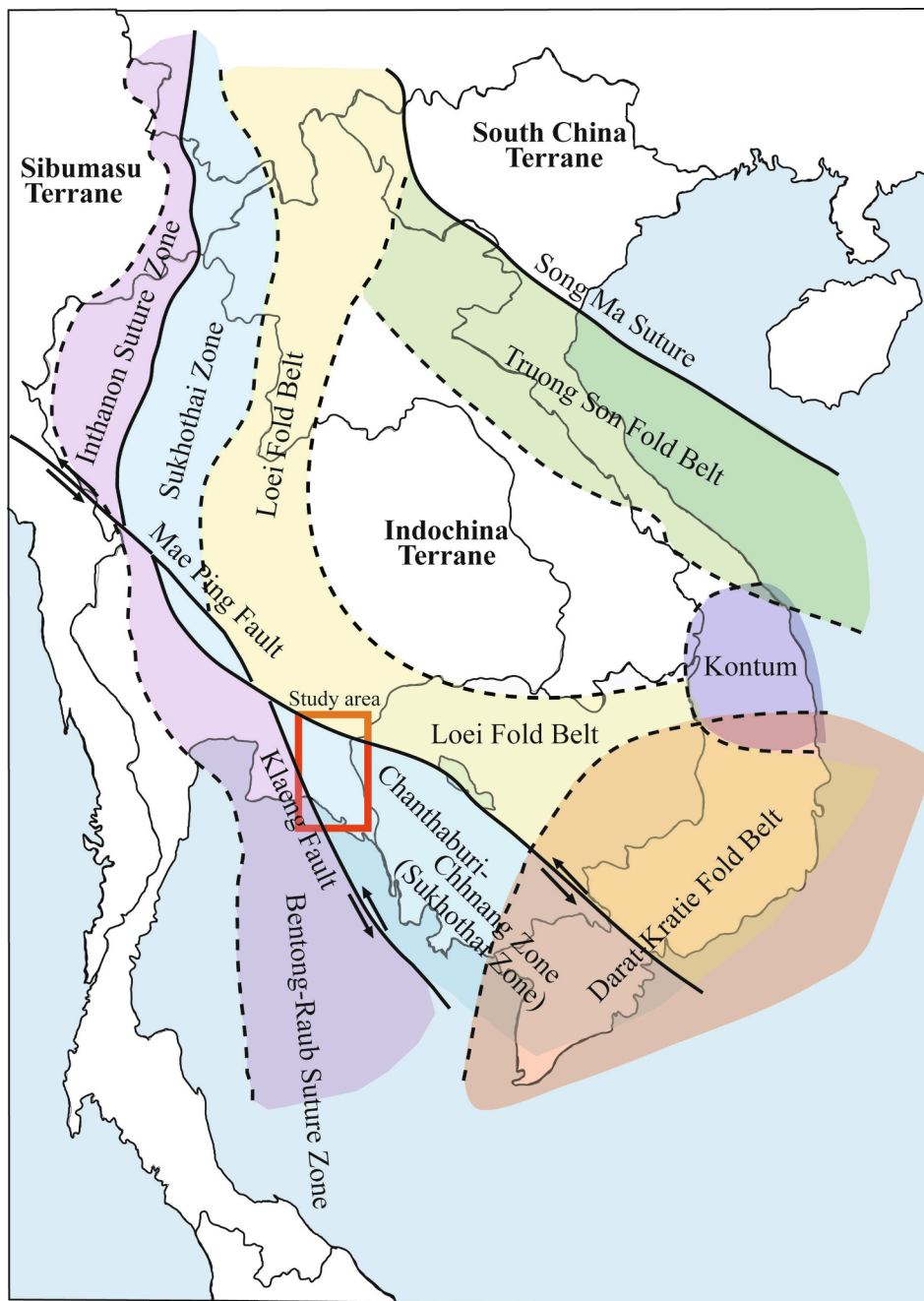
Fig. 12. Simplified tectonic map of Southeast Asia. Data obtained from Sone and Metcalfe (2013), Wang, et al., (2016), Cheng et al. (2019), Kasahara et al. (2021), and this study.

body shows a relatively young zircon U-Pb age of 55 Ma, which is likely related to the collision of the Indian continent with the Eurasian continent.

The magnetic, geochemical and radiogenic isotopic signatures of the Chanthaburi, Pliew, Klathing, Khao Cha Mao, and Khao Hin Son granite bodies are very similar to those of the granites in southwestern Cambodia (Cheng et al., 2019). The study area can therefore be considered as an extensional area of southwestern Cambodia to Thailand. This suggests that the study area belongs to the Sukhothai Zone (the Chanthaburi-Kampong Chhnang Zone).

CRediT authorship contribution statement

Declaration of Competing Interest

The authors declare that they have no known competing financial interests or personal relationships that could have appeared to influence the work reported in this paper.

Acknowledgements

Appendix A. Supplementary material

Supplementary data to this article can be found online at https://doi.org/10.1016/j.jaesx.2022.100111.

References

Azadbakht, Z., Rogers, N., Lentz, D.R., McFarlane, C.R.M., 2019. Petrogenesis and associated mineralization of Acadian related granitoids in New Brunswick. In: Targeted Geoscience Initiative: 2018 Report of Activities. Geological Survey of Canada, Ottawa, pp. 243–278.

Bunopas, S., 1981. Paleogeographic history of western Thailand and adjacent parts of South-East Asia: A plate tectonics interpretation. Geol. Surv. Sp. Publ., Thailand 5, 810p.

Burrett, C., Khin Zaw, Meffre, S., Lai, C.K., Khositanont, S., Chaodumrong, P., Udchachon, M., Ekins, S., Halpin, J., 2014. The configuration of Greater Gondwana-Evidence from LA ICPMS, U-Pb geochronology of detrital zircons from the Palaeozoic and Mesozoic of Southeast Asia and China. Gondwana Res. 26 (1), 31–51.

Charusiri, P., Clark, A.H., Farrar, E., Archibald, D., Charusiri, B., 1993. Granite belts in Thailand: evidence from the ^{40}Ar/^{39}Ar geochronological and geologic syntheses. J. Asian Earth Sci. 8, 127–136.

Charusiri, P., Pongsapitch, W., Daorerk, V., Charusiri, B., 1992. Anatomy of Chanthaburi granitoids: geochronology, petrochemistry, tectonics, and associated mineralization. In: Piancharoen, C. (Ed.), Proceedings of the National Conference on Geologic Resources of Thailand: Potential for Future Development. Department of Mineral Resources, Ministry of Industry, Bangkok, Thailand, pp. 383–392.

Cheng, R., Uchida, E., Katayose, M., Yarimizu, K., Shin, K.-C., Kong, S., Nakano, T., 2019. Petrogenesis and tectonic setting of Late Paleozoic to Late Mesozoic igneous rocks in Cambodia. J. Asian Earth Sci. 185 (104046), 1–21.

Cobbing, E.J., Mallick, D.I.J., Pitfield, P.E.J., Teoh, L.H., 1986. The granites of the Southeast Asian Tin Belt. J. Geol. Soc., London 143 (3), 537–550.

Cox, K.G., Bell, J.D., Pankhurst, R.J., 1979. The Interpretation of Igneous Rocks. Allen and Unwin, London, p. 450.

DePaolo, D.J., Wasserburg, G.J., 1979. Petrogenetic mixing models and Nd-Sr isotope patterns. Geochim. Cosmochim. Acta 43, 615–627.

Faure, G., Mensing, T.M., 2005. Isotopes – Principles and applications, 3rd ed. John Wiley & Sons Hoboken, New Jersey, USA, pp. 347–411.

Faure, M., Nguyen, V.V., Hoai, L.T.T., Lepvrier, C., 2018. Early Paleozoic or Early-Middle Triassic collision between the South China and Indochina Blocks: The Controversy resolved? Structural insights from the Kon Tum Massif (Central Vietnam). J. Asian Earth Sci. 166, 162–180.

Ferrari, O.M., Hochard, C., Stampfli, G.M., 2008. An alternative plate tectonic model for the Palaeozoic-Early Mesozoic Palaeotethyan evolution of Southeast Asia (Northern Thailand–Burma). Tectonophys. 451 (1-4), 346–365.

Gardiner, N.J., Searle, M.P., Robb, L.J., Morley, C.K., 2015. Neo-Tethyan magmatism and metallogeny in Myanmar – An Andean analogue? J. Asian Earth Sci. 106, 197–215.

Ishihara, S., 1981. The granitoid series and mineralization. In: Skinner, B.J. (Ed.), Economic Geology Seventy-Fifth Anniversary Volume. Economic Geology Publishing Company, Pennsylvania, pp. 458–484.

Jackson, S.E., Pearson, N.J., Griffin, W.L., Belousova, E.A., 2004. The application of laser ablation-inductively coupled plasma-mass spectrometry to in situ U-Pb zircon geochronology. Chem. Geol. 211 (1-2), 47–69.

Jochum, K.P., Brueckner, S.M., 2008. Reference materials in geoanalytical and environmental research - review for 2006 and 2007. Geostand. Geoanal. Res. 32 (4), 405–452.

Kamvong, T., Khin Zaw, Meffre, S., Maas, R., Stein, H., Lai, C.-K., 2014. Adakites in the Truong Son and Loei fold belts, Thailand and Laos: Genesis and implications for geodynamics and metallogeny. Gondwana Res. 26 (1), 165–184.

Kanjanapayont, P., Kieduppatum, P., Klötzli, U., Klötzli, E., Charusiri, P., 2013. Deformation history and U–Pb zircon geochronology of the high-grade metamorphic rocks within the Klaeng fault zone, eastern Thailand. J. Asian Earth Sci. 77, 224-233.

Kasahara, N., Niki, S., Uchida, E., Yarimizu, K., Cheng, R., Hirata, T., 2021. Zircon U–Pb chronology on plutonic rocks from northeastern Cambodia. Heliyon 7, e06752, 1-12.

Khin Zaw, Meffre, S., Lai, C.-K., Burrett, C., Santosh, M., Graham, I., Manaka, T., Salam, A., Kamvong, T., Cromie, P., 2014. Tectonics and metallogeny of mainland Southeast Asia — A review and contribution. Gondwana Res. 26 (1), 5–30.

Ludwig, K.R., 1998. On the treatment of concordant uranium-lead ages. Geochim. Cosmochim. Acta 62 (4), 665–676.

Manaka, T., Khin Zaw, Meffre, S., Vasconcelos, P.M., Golding, S.D., 2014. The Ban Houayxai epithermal Au-Ag deposit in the Northern Lao PDR: Mineralization related to the Early Permian arc magmatism of the Truong Son Fold Belt. Gondwana Res. 26 (1), 185–197.

Mantajit, N., Hintong, C., 1999. Geological map of Thailand: scale 1: 2,500,000. Geological Survey Division, Department of Mineral Resources, Bangkok, Thailand.

McDonough, W.F., Sun, S.S., 1995. The composition of the Earth. Chem. Geol. 120, 223–253.

Metcalfe, I., 1984. Stratigraphy, palaeontology and palaeogeography of the Carboniferous of Southeast Asia. Mem. Soc. Geol. France 147, 107–118.

Metcalfe, I., 2011. Palaeozoic-Mesozoic history of SE Asia. Geological Society, London, Special Publications 355 (1), 7–35.

Metcalfe, I., 2013. Gondwana dispersion and Asian accretion: Tectonic and palaeogeographic evolution of eastern Tethys. J. Asian Earth Sci. 66, 1–33.

Middlemost, E.A.K., 1994. Naming materials in the magma/igneous rock system. Earth Sci. Rev. 37 (3-4), 215–224.

Morley, C.K., 2012. Earth-science reviews late cretaceous – early palaeogene tectonic development of SE Asia. Earth Sci. Rev. 115 (1-2), 37–75.

Morley, C.K., Ampaiwan, P., Thanudamrong, S., Kuenphan, N., Warren, J., 2013. Development of the Khao Khwang Fold and Thrust Belt: Implications for the geodynamic setting of Thailand and Cambodia during the Indosinian Orogeny. J. Asian Earth Sci. 62, 705–719.

Nachtergaele, S., Glorie, S., Morley, C., Charusiri, P., Kanjanapayont, P., Vermeesch, P., Carter, A., Van Ranst, G., De Grave, J., 2020. Cenozoic tectonic evolution of southeastern Thailand derived from low-temperature thermochronology. J. Geol. Soc. 177 (2), 395–411.

Nualkhao, P., Takahashi, R., Imai, A., Charusiri, P., 2018. Petrochemistry of granitoids along the Loei Fold Belt, Northeastern Thailand. Resour. Geol. 68 (4), 395–424.

Pearce, J.A., Harris, N.B.W., Tindle, A.G., 1984. Trace element distribution diagrams for the tectonic interpretation of granitic rocks. J. Petrol. 25, 956–983.

Rossignol, C., Bourquin, S., Hallot, E., Poujol, M., Dabard, M.-P., Martini, R., Villeneuve, M., Cornée, J.-J., Brayard, A., Roger, F., 2018. The Indosinian orogeny: a perspective from sedimentary archives of north Vietnam. J. Asian Earth Sci. 158, 352–380.

Rudnick, R.L., Gao, S., 2005. Composition of the continental crust. In The Crust, Editor Rudnick, R.L., Elsevier, Amsterdam, Treatise on Geochemistry Vol. 3, pp.1–64.

Sakata, S., Hirakawa, S., Iwao, H., Danhara, T., Guillong, M., Hirata, T., 2017. A new approach for constraining the magnitude of initial disequilibrium in Quaternary zircon by coupled uranium and thorium decay series dating. Quat. Geochronol. 38, 1–12.

Salam, A., Zaw, K., Meffre, S., McPhie, J., Lai, C.-K., 2014. Geochemistry and geochronology of the Chatree epithermal gold–silver deposit: Implications for the tectonic setting of the Loei Fold Belt. Central Thailand. Gondwana Res. 26 (1), 198–217.

Sanematsu, K., Murakami, H., Duangsurigna, S., Vilayhack, S., Duncan, R.A., Watanabe, Y., 2011. ^{40}Ar/^{39}Ar ages of granitoids from the Truong Son fold belt and Kontum massif in Laos. J. Mineral. Petrol. Sci. 106 (1), 13–25.

Searle, M.P., Whitehouse, M.J., Robb, L.J., Ghani, A.A., Hutchison, C.S., Sone, M., Ng, S.-W.-P., Roselee, M.H., Chung, S.-L., Oliver, G.J.H., 2012. Tectonic evolution of the Sibumasu-Indochina terrane collision zone in Thailand and Malaysia: constraints from new U-Pb zircon chronology of SE Asian tin granitoids. J. Geol. Soc. 169 (4), 489–500.

Schaefer, B.F., 2016. Radiogenic Isotope Geochemistry. Oxford University Press, United Kingdom, pp. 40–56, 145–176.

Shellnutt, J.G., Lan, C.Y., Long, T.V., Usuki, T., Yang, H.J., Mertzman, S.A., Iizuka, Y., Chung, S.L., Wang, K.L., Hsu, W.Y., 2013. Formation of Cretaceous Cordilleran and post-orogenic granites and their microgranular enclaves from the Datat zone, southern Vietnam: Tectonic implications for the evolution of Southeast Asia. Lithos 182–183, 229–241.

Shi, M., Zaw Khin, Liu, S., Xu, B., Meffre, S., Cong, F., Nie, F., Peng, Z., Wu, Z., 2021. Geochronology and petrogenesis of Carboniferous and Triassic volcanic rocks in NW Laos: Implications for the tectonic evolution of the Loei Fold Belt. J. Asian Earth Sci. 208, 104661. https://doi.org/10.1016/j.jseaes.2020.104661.

Shin, K.C., Kurosawa, M., Anma, R., Nakano, T., 2009. Genesis and mixing/mingling of mafic and felsic magmas of back arc granite: Miocene Tsushima pluton, Southeast Japan. Resour. Geol. 59, 25–50.

Sone, M., Metcalfe, I., 2008. Parallel Tethyan sutures in mainland Southeast Asia: New insights for Paleo-Tethys closure and implications for the Indosinian orogeny. Comptes Rendus Geosci. 340, 166–179.

Sone, M., Metcalfe, I., Chaodumrong, P., 2012. The Chanthaburi terrane of southeastern Thailand: Stratigraphic confirmation as a disrupted segment of the Sukhothai Arc. J. Asian Earth Sci. 61, 16–32.

Tanaka, T., Togashi, S., Kamioka, H., Amakawa, H., Kagami, H., Hamamoto, T., Yuhara, M., Orihashi, Y., Yoneda, S., Shimizu, H., Kunimaru, T., Takahashi, K., Yanagi, T., Nakano, T., Fujimaki, H., Shinjo, R., Asahara, Y., Tanimizu, M., Dragusanu, C., 2000. JNdi-1: a neodymium isotopic reference in consistency with LaJolla neodymium. Chem. Geol. 168 (3-4), 279–281.

Thuy, T.B.N., Satir, M., Siebel, W., Chen, F., 2004. Granitoids in the Dalat zone, southern Vietnam: age constrains on magmatism and regional geological implications. Int. J. Earth Sci. 93, 329–340.

Tien, P.C., An, L.D., Bach, L.D., Bac, D.D., Vongdara, B., Phengthavongsa, B., Danh, T., Dy, N.D., Dung, H.T., Hai, T.Q., Khuc, V., Kun, S.C., Long, P.D., Ly, M.N., My, N.Q., Ngan, P K., Ngoc, N., Ratanavong, N., Quoc, N.K., Quyen, N.V., Aphaymani, S.D., Thanh, T.D., Tri, T.V., Truyen, M.T., and Xay, T.S., 1990. Geology of Cambodia, Laos

and Vietnam. Explanatory note to the geological map of Cambodia, Laos and Vietnam at 1: 1,000,000 scale. The Geological Survey of Vietnam, Hanoi.

Uchida, E., Osada, K., Nakao, K., 2017. Major and trace element chemical compositional signatures of some granitic rocks related to metal mineralization in Japan. Open Jour. Geol. 07 (04), 559–576.

Ueno, K., Hisada, K.-I., 2001. The Nan–Uttaradit–Sa Kaeo Suture as a main Paleo-Tethyan suture in Thailand: is it real? Gondwana Res. 4 (4), 804–806.

Veeravinantanakul, A., Takahashi, R., Agangi, A., Ohba, T., Watanabe, Y., Elburg, M.A., Ueckermann, H., Kanjanapayont, P., Charusiri, P., 2021. Zircon Hf-isotope constraints on the formation of metallic mineral deposits in Thailand. Resour. Geol. 71 (4), 436–469.

Vermeesch, P., 2018. IsoplotR: A free and open toolbox for geochronology. Geosci. Front 9 (5), 1479–1493.

Wang, Y., He, H., Cawood, P.A., Srithai, B., Feng, Q., Fan, W., Zhang, Y., Qiana, X., 2016. Geochronological, elemental and Sr-Nd-Hf-O isotopic constrains on the petrogenesis

of the Triassic post-collisional granitic rocks in NW Thailand and its Paleotethyan implications. Lithos 266–267, 264–286.

Whalen, J.B., Currie, K.L., Chappell, B.W., 1987. A-type granites: geochemical characteristics, discrimination and petrogenesis. Contrib. Miner. Petrol. 95 (4), 407–419.

Wilson, M., 1989. A Global Tectonic Approach. Unwin Hyman, London, p. 466p.

Further reading

Yang, X.-M., Lentz, D.R., Chi, G., Thorne, K.G., 2008. Geochemical characteristics of gold-related granitoids in southwestern. New Brunswick. Canada. Lithos 104 (1-4), 355–377.